

Noise correction in gene expression data: A new approach based on subspace method

Nader Alharbi*, Zara Ghodsi*, Hossein Hassani *

**The Statistical Research Centre, Bournemouth University,
89 Holdenhurst Road, Bournemouth BH8 8EB, UK*

Abstract

We present a new approach for removing the nonspecific noise from *Drosophila* segmentation genes. The algorithm used for filtering here is an enhanced version of Singular Spectrum Analysis (SSA) method which decomposes a gene profile into the sum of a signal and noise. Since the main issue in extracting signal using SSA procedure lies in identifying the number of eigenvalues needed for signal reconstruction, this paper seeks to explore the applicability of the new proposed method for eigenvalues identification in four different gene expression profiles. Our findings indicate that when extracting signal from different genes, for optimised signal and noise separation, different number of eigenvalues need to be chosen for each gene.

1 Introduction

Segmentation in *Drosophila melanogaster* is arguably the best studied example of gene regulatory network in developmental studies [1]. In this network, it is widely accepted that the patterns of the segmentation factors which have been activated by the primary morphogens direct the early embryo development. However, due to the presence of noise, finding the pattern of segmentation factors is not a simple task [2–4] and even a small level of noise in gene expression patterns will considerably affect our understanding of the embryo developmental fate. Hence, it is important to probe the gene expression signal using a method which effectively enables us to filter the fluctuations of the related gene protein profile.

These profiles can mostly be achieved by using fluorescence imaging technique [5]. Such quantification relies on the assumption that the actual protein concentrations detected by the Fluorescence in situ hybridization (FISH) technique are linearly related to the embryos natural protein concentration. However, the obtained profile contains different levels of noise which need to be removed first. Among several noise removal models Singular Spectrum Analysis (SSA) is a relatively new method which has recently transformed itself into a valuable tool for gene expression signal extraction. The first such application of SSA was seen in 2006 when Holloway et al. studied the relation

36 between maternal protein gradients and segmentation process in *Drosophila*,
 37 by analysing gene expression patterns extracted by SSA [6]. It is worthy to
 38 mention two powerful characteristics of SSA; no requirement of any assump-
 39 tions about the data and related residuals and its effective performance in noise
 40 filtering [7] made SSA a valuable method in analysing segmentation genes pro-
 41 file. Since then SSA and related theoretical developments of this method such
 42 as two-dimensional SSA and SSA based on minimum variance has been used
 43 in several other studies, see for example [3, 5, 8–13].

44 Even though the signal extraction by SSA appears to be simple, in practice
 45 it is a complicated task since for some cases the trend cannot be separated from
 46 noise or cyclic components just by choosing the first eigenvalue. This issue for
 47 the first time raised by Alexandrov et al. in [3] in which the author suggested
 48 using either a small window length or adding a constant to the series for im-
 49 proving the separability between signal and noise [3]. Although the practical
 50 possibility of these suggestions there is still an open question related with the
 51 identification of the number of eigenvalues required for series reconstruction.

52 To address this question we mainly follow the idea proposed in [14–16]. The
 53 proposed method has been mainly used for noise reduction, filtering, signal
 54 extraction and distinguishing chaos from noise in time series analysis [17]. In
 55 identifying the number of the eigenvalues this method mainly relies on the dis-
 56 tribution of the scaled Hankel matrix eigenvalues. Here, we apply the method
 57 for signal extraction in four different genes; bicoid (bcd), caudal (cad), giant
 58 (gt) and even-skipped (eve) which are among the most important zygotic seg-
 59 mentation genes. The approach enables us to decide the appropriate number
 60 of eigenvalues related to the gene signal.

61 The remainder of this paper is organised such that Section 2 describe the
 62 methodology which is followed by the empirical results from the simulated
 63 and real data applications in Section 3. The paper concludes with a concise
 64 summary in Section 4.

65 2 Methodology

66 2.1 A brief description

67 Presented below is a short description of the method used in this study. The
 68 main aim of the SSA technique is to analyse the original series into a sum of
 69 series, so that each component can be identified as either a main component
 70 or noise. Our interest here is to consider the signal as a whole so that we can
 71 determine the eigenvalues related to the signal component. The SSA approach
 72 consists of two main stages: decomposition and reconstruction; of which each
 73 stage consists of two compatible steps. Embedding and singular value decom-
 74 position (SVD) in the first stage, grouping and diagonal averaging in the second
 75 stage [7]. The proposed approach is a novel step that can be used between the
 76 first and second stages of SSA to select the proper value of eigenvalues r .

In doing so, let us consider a one-dimensional series $Y_N = (y_1, \dots, y_N)$ of
 length N . Mapping this series into a multi-dimensional series X_1, \dots, X_K
 where $X_i = (y_i, \dots, y_{i+L-1})^T \in \mathbf{R}^L$ provides $\mathbf{X} = (x_{i,j})_{i,j=1}^{L,K}$, where L ($2 \leq$

$L \leq N/2$) and $K = N - L + 1$. The matrix \mathbf{X} is a Hankel matrix, which means all the elements along the diagonal $i + j = \text{const}$ are equal. Set $\mathbf{A} = \mathbf{X}\mathbf{X}^T$ and denote by λ_i ($i = 1, \dots, L$) the eigenvalues of \mathbf{A} taken in the decreasing order of magnitude ($\lambda_1 \geq \dots \geq \lambda_L \geq 0$) and by U_1, \dots, U_L the orthonormal system of the eigenvectors of the matrix \mathbf{A} corresponding to these eigenvalues. Set

$$d = \text{rank } \mathbf{X} = \max(i, \text{ such that } \lambda_i > 0).$$

The SVD of the trajectory matrix can be written as:

$$\mathbf{X} = \mathbf{X}_1 + \dots + \mathbf{X}_d, \quad (1)$$

77 where $\mathbf{X}_i = \sqrt{\lambda_i} U_i V_i^T$. The elementary matrices \mathbf{X}_i have rank 1, U_i and V_i
78 are the left and right eigenvectors of the trajectory matrix. Note that the
79 collection $(\sqrt{\lambda_i}, U_i, V_i)$ is called the i th eigentriple of the SVD. Note also that
80 $\|\mathbf{X}\|_F^2 = \text{tr}(\mathbf{X}\mathbf{X}^T) = \sum_{i=1}^L \lambda_i$ and $\|\mathbf{X}_i\| = \lambda_i$, where $\|\cdot\|_F$ denotes the Frobenius
81 norm.

82 Let us now consider the step that comes between the two stages in SSA,
83 that is to divide the matrix \mathbf{A} by its trace, $\mathbf{A}/\text{tr}(\mathbf{A})$. Let ζ_1, \dots, ζ_L denote
84 the eigenvalues of the matrix $\mathbf{A}/\text{tr}(\mathbf{A})$ in decreasing order of magnitude ($1 \geq$
85 $\zeta_1 \geq \dots \geq \zeta_L \geq 0$). In this step, we perform the simulation technique to gain
86 the distribution of ζ_i , so we can understand the behaviour of each eigenvalue,
87 which can be useful for obtaining the proper value of r . In this paper, our
88 aim is to ascertain the distribution of ζ_i and its related forms that can be used
89 directly for choosing the optimal value of r for the genes signal extraction.

Once r is obtained, the grouping step splits the matrices \mathbf{X}_i into two groups. Therefore, (1) can be written as

$$\mathbf{X} = \mathbf{S} + \mathbf{E}, \quad (2)$$

90 where $\mathbf{S} = \sum_{i=1}^r \mathbf{X}_i$ is the signal matrix and $\mathbf{E} = \sum_{i=r+1}^d \mathbf{X}_i$ is the noise matrix.

91 At the final step, we use the diagonal averaging to transform the matrix \mathbf{S} into
92 a new series of length N (for more information see [18, 19]).

93 2.2 Algorithm

94 The Algorithm is divided in two stages. At the first stage, we use skewness
95 coefficient and coefficient of variation of ζ_i as the main indicators to find the
96 optimal value of r for the separability between signal and noise, and then at
97 the second stage, we reconstruct the time series.

98 2.2.1 Stage 1:

- 99 1. Transfer a one-dimensional time series $Y_N = (y_1, \dots, y_N)$ into the multi-
100 dimensional series X_1, \dots, X_K with vectors $X_i = (y_i, \dots, y_{i+L-1})^T \in$
101 \mathbf{R}^L , where $K = N - L + 1$, and the window length L is an integer
102 such that $2 \leq L \leq N/2$. This steps provides the trajectory matrix
103 $\mathbf{X} = [X_1, \dots, X_K] = (x_{ij})_{i,j=1}^{L,K}$.

- 104 2. Computing the matrix $\mathbf{A} = \mathbf{X}\mathbf{X}^T / \text{tr}(\mathbf{X}\mathbf{X}^T)$.
- 105 3. Compute the eigenvalues and eigenvectors of the matrix \mathbf{A} and represent
106 it in the form $\mathbf{A} = \mathbf{P}\mathbf{\Gamma}\mathbf{P}^T$. Here, $\mathbf{\Gamma} = \text{diag}(\zeta_1, \dots, \zeta_L)$ is the diagonal
107 matrix of the eigenvalues of \mathbf{A} that has the order $(1 \geq \zeta_1 \geq \zeta_2, \dots, \zeta_L \geq 0)$
108 and $\mathbf{P} = (P_1, P_2, \dots, P_L)$ is the corresponding orthogonal matrix of the
109 eigenvectors of \mathbf{A} .
- 110 4. Simulate the original series m times and calculate the eigenvalues for
111 each series. We simulate y_i from a uniform distribution with boundaries
112 $y_i - a$ and $y_i + b$, where $a = |y_{i-1} - y_i|$ and $b = |y_i - y_{i+1}|$. In order to
113 obtain a noisy series similar to the real one, random error ϵ with a normal
114 distribution with zero mean and variance σ_ϵ^2 with different amplitudes
115 were added to different part of the series.
- 116 5. Calculate the coefficient of skewness for each eigenvalue, $\text{skew}(\zeta_i)$. If
117 $\text{skew}(\zeta_c)$ is the maximum, then select $r = c - 1$.
- 118 6. Calculate the coefficient of variation, $CV(\zeta_i)$. This can split the eigenval-
119 ues in two groups, from ζ_1 to ζ_{c-1} which are corresponding to the signal
120 and the rest which has almost a U shape which are corresponding to the
121 noise component.
- 122 7. Calculate the absolute values of the correlation between ζ_i and ζ_{i+1} , and
123 plot them in one figure. If $\rho(\zeta_{c-1}, \zeta_c)$ is the minimum, and the pattern
124 for $\rho(\zeta_c, \zeta_{c+1})$ to $\rho(\zeta_{L-1}, \zeta_L)$ has the same pattern for the white noise,
125 then choose $r = c - 1$.

126 2.2.2 Stage 2

- 127 1. Use the number of the eigenvalues r obtained in the first stage to calculate
128 the approximated signal matrix $\tilde{\mathbf{S}}$, that is $\tilde{\mathbf{S}} = \sum_{i=1}^r \mathbf{X}_i$, where $\mathbf{X}_i =$
129 $\sqrt{\lambda_i} U_i V_i^T$, U_i and V_i stands for the left and right eigenvectors of the
130 trajectory matrix.
- 131 2. Transition to the one dimensional series can now be achieved by averaging
132 over the diagonals of the matrix $\tilde{\mathbf{S}}$.

133 3 Real data

134 3.1 Data description

135 The gene expression data in wild-type *Drosophila melanogaster* embryos achieved
136 by fluorescently tagged antibodies technique and is available via [20] where a
137 more detailed description on the biological characteristics, method and data is
138 made available. This data was extracted from the nuclear intensities of %10
139 longitudinal strips and the data was not processed for any other noise removal.

140 Of the many segmentation genes, we are only concerned with four different
141 genes in this study; *bcd*, *cad*, *gt* and *eve* which among them *bcd* is maternal

142 and, *cad* has both maternal and zygotic origin and *gt* and *eve* are respectively
 143 related to gap and pair rule categories of zygotic genes [5, 6, 8].

144 *bcd* mRNA is completely maternal and the Bcd protein gradient is formed at
 145 cleavage cycle 9 [5, 6, 8]. Figure 1(a) depicts a typical example of *Bcd* gradient
 146 related to cleavage cycle 14(3). Although this figure suggests *Bcd* follows an
 147 exponential trend due to the high volatility seen in the series, the extraction of
 148 this trend is not a simple task.

149 *cad* mRNA has both maternal and zygotic origin and the maternal trans-
 150 cripts begin to translate immediately after fertilization. However, proteins
 151 encoded by *gt* and *eve* were reported to appear at cycle 12 and 10 respectively
 152 and it is accepted that the posterior stripe of *gt* expression is regulated by *bcd*
 153 and *cad* [5, 6, 8, 21].

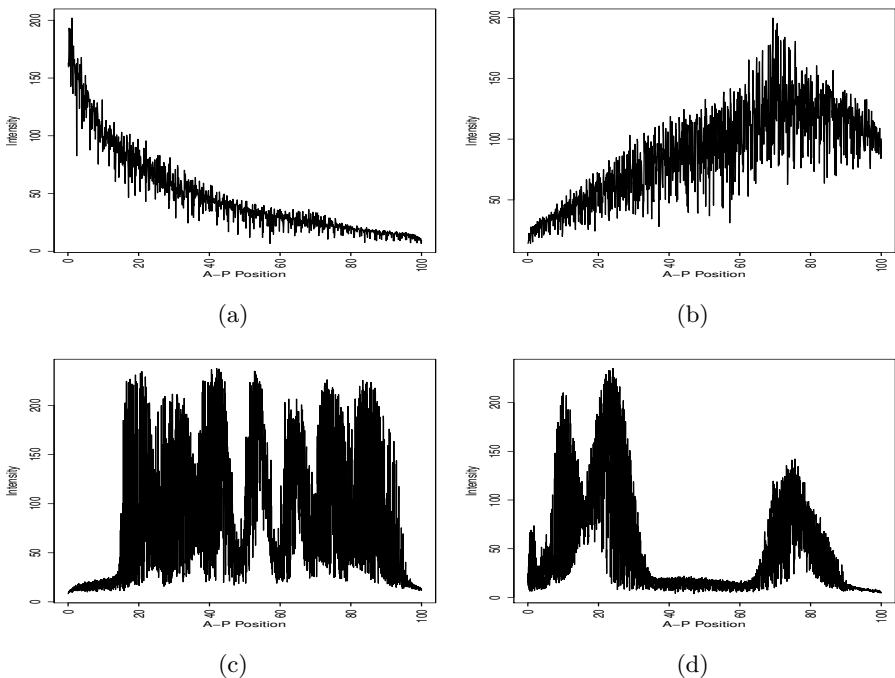


Figure 1: Experimental data from *Drosophila melanogaster* embryo; (a): *bcd*,
 (b): *cad*, (c): *eve*, (d): *gt* .

154 3.2 Main results

155 In this paper, a series of simulated data are used to evaluate the performance of
 156 the newly introduced approach. To generate the simulated noisy profiles with
 157 similar structure, shape and distribution to the real gene expression profiles
 158 we mainly follow the algorithm presented in [17, 18]. This algorithm has also
 159 been explained briefly in Section 2.2. Although the gene expression profiles
 160 are slightly different from embryo to embryo, as the obtained results in terms
 161 of number of eigenvalues are similar, we only consider ten different embryos

162 for studying each gene. In this regard, each copy of gene expression data was
 163 simulated 10^4 times. Studying the distribution of each eigenvalue provides the
 164 capacity to obtain an accurate and deep intuitive understanding of selecting
 165 the proper value of r . The first data for each gene is analysed and discussed in
 166 more detail whilst the results of the other data are summarised based on the
 167 outcomes of the skewness, variation and correlation coefficients. The window
 168 length used for analysing the *bcd*, *cad*, *gt* and *eve* genes series is 200 (for more
 169 information for the selection of the window length refer to [22]).

We mainly focus on the third moment, that is the skewness of the distribution for each eigenvalue:

$$skew(\zeta_i) = \frac{\frac{1}{m} \sum_{n=1}^m (\zeta_{i,n} - \bar{\zeta}_i)^3}{\left[\frac{1}{m-1} \sum_{n=1}^m (\zeta_{i,n} - \bar{\zeta}_i)^2 \right]^{3/2}}, \quad (3)$$

and the coefficient of variation, $CV(\zeta_i)$, which is defined as the ratio of the standard deviation $\sigma(\zeta_i)$ and $\bar{\zeta}_i$:

$$CV_i = \frac{\sigma(\zeta_i)}{\bar{\zeta}_i}. \quad (4)$$

170 In addition, the Spearman correlation ρ between ζ_i and ζ_{i+1} is also evaluated
 171 to enhance the results obtained by *skew* and *CV* measures. The absolute value
 172 of the correlation between ζ_i and ζ_{i+1} is considered, 1 indicates that ζ_i and ζ_{i+1}
 173 have perfect positive correlation whilst 0 shows there is no correlation between
 174 them.

175 Figure 2 illustrates the results of $skew(\zeta_i)$ (left) and $CV(\zeta_i)$ (right) for the
 176 first data series for each gene type. It can be seen from the left column that the
 177 maximum value of *skew* is obtained for ζ_2 in both *bcd* and *cad* data. Whereas,
 178 $skew(\zeta_4)$ is the maximum for both *eve* and *gt* series. In the right column,
 179 the results of *CV* splits the eigenvalues into two groups for each data; the
 180 second group looks like a U shape which is related to the noise component.
 181 The results indicate that $r = 2, 2, 3, 3$ for extracting the *bcd*, *cad*, *eve* and *gt*
 182 signal, respectively.

183 Furthermore, the result of ρ can be used as a decision or test tool if the *skew*
 184 and *CV* measures give different results. However, in these typical examples,
 185 the results of those two measures are the same which also supported by the
 186 results of the correlation coefficient. It is obvious that the minimum value of ρ
 187 are emerged between (ζ_2, ζ_3) , (ζ_2, ζ_3) , (ζ_3, ζ_4) and (ζ_3, ζ_4) for *bcd*, *cad*, *eve* and
 188 *gt*, respectively. Therefore, the results enhance that $r = 2, 2, 3, 3$ for the first
 189 data for each gene (see Fig. 3).

190 Tables. 1, 2, 3, and 4 depict the results of r based on those three measures
 191 for all 40 series. For the *bcd* signal extraction, all the outputs show $r = 2$ for
 192 all *bcd* data (see Table. 1). Similar results was emerged for extracting the *cad*
 193 signal, most of the outcomes indicate $r = 2$.

194 For the *eve* data, $r = 3$ for five series as all the three measures give the
 195 same result. However, for example; for series 2, the results of *skew* and *CV*
 196 are different, $r = 3$ and $r = 4$, respectively. To overcome this, we look at the

197 result of ρ , which confirms $r = 4$. In this regards, the decision that $r = 3$ is
 198 for six series of ten *eve* data. Table. 4 demonstrates that $r = 3$ for all *gt* series
 199 except the last series, because all measures have the same results. As a result,
 200 for $L = 200$, the required eigenvalues to extract the *bcd*, *cad*, *eve*, and *gt* signals
 201 are 2, 2, 3, 3, respectively. Table. 5 shows the final results for all four genes
 202 along with the most frequent reported *skew*, *CV* and ρ .

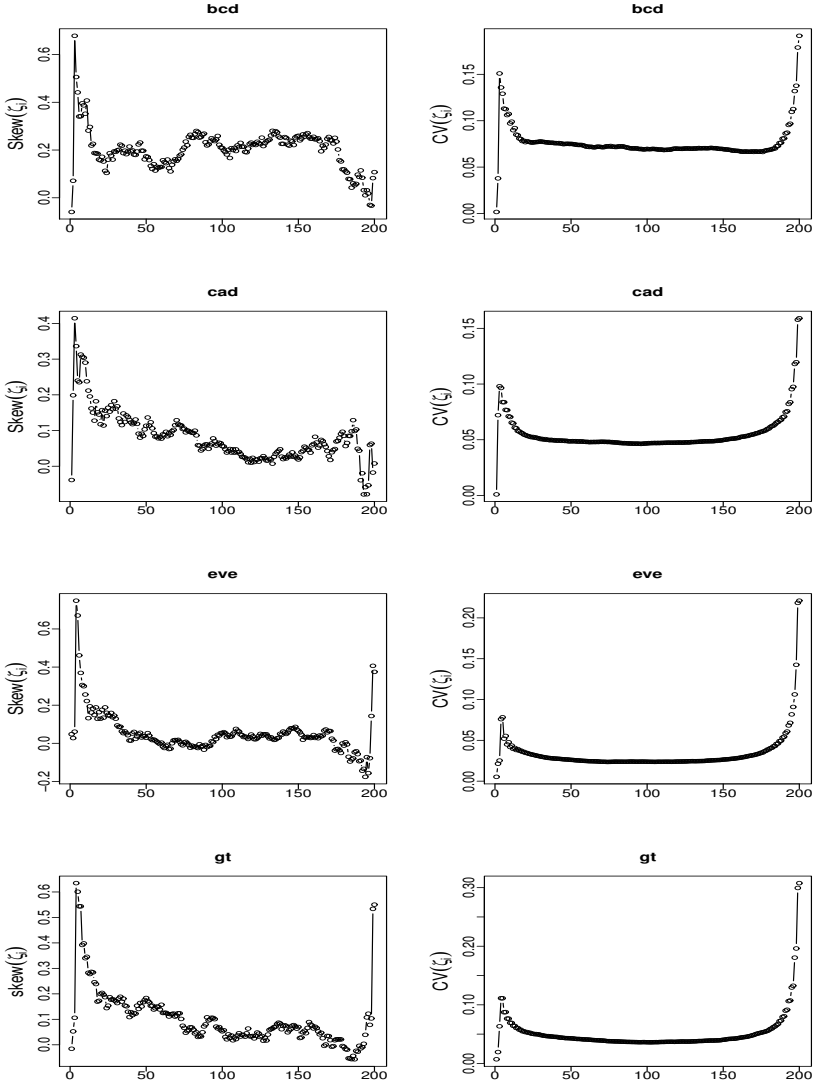


Figure 2: The skewness coefficient (left) and the variation coefficient of ζ_i (right) for the first series of *bcd*, *cad*, *gt* and *eve* data.

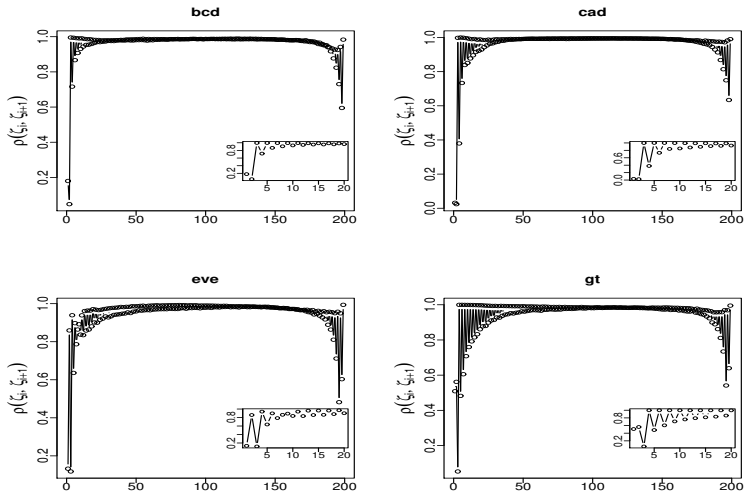


Figure 3: The correlation between ζ_i and ζ_{i+1} for the first series from each data.

Table 1: The values of r based on *Skew* and *CV* for the ten *bcd* series.

Series	$r(skew)$	$r(CV)$	$r(\rho)$	Series	$r(skew)$	$r(CV)$	$r(\rho)$
1	2	2	2	6	2	2	2
2	2	2	2	7	2	2	2
3	2	2	2	8	2	2	2
4	2	2	2	9	2	2	2
5	2	2	2	10	4	2	2

Table 2: The values of r based on *skew* and *CV* for the ten *cad* series.

Series	$r(skew)$	$r(CV)$	$r(\rho)$	Series	$r(skew)$	$r(CV)$	$r(\rho)$
1	2	2	2	6	1	2	1
2	2	2	2	7	2	2	2
3	2	2	2	8	2	2	2
4	1	2	1	9	2	1	2
5	2	2	2	10	3	3	3

203 After the step of identifying the value of r , we can use those leader eigenvalues
 204 in the second stage of the SSA approach (Grouping and Diagonal averaging)
 205 to reconstruct the first typical data for each gene. Fig. 4 shows the result
 206 of the gene signal extraction or reconstruction series without noise. The red
 207 and the black lines correspond to the reconstructed series and the original series
 208 respectively. As a results, the considered r for the reconstruction of the original
 209 series is obtained properly.

Table 3: The values of r based on $skew$ and CV for the ten *eve* series.

Series	$r(skew)$	$r(CV)$	$r(\rho)$	Series	$r(skew)$	$r(CV)$	$r(\rho)$
1	3	3	3	6	3	4	4
2	4	3	4	7	3	3	3
3	6	6	6	8	4	4	4
4	6	4	4	9	3	3	3
5	3	3	3	10	3	3	3

Table 4: The values of r based on $skew$ and CV for the ten *gt* series.

Series	$r(skew)$	$r(CV)$	$r(\rho)$	Series	$r(skew)$	$r(CV)$	$r(\rho)$
1	3	3	3	6	3	3	3
2	3	3	3	7	3	3	3
3	3	3	3	8	3	3	3
4	3	3	3	9	3	3	3
5	3	3	3	10	5	3	5

Table 5: The final result obtained in noise-signal separation study.

Gene type	$r(skew)$	$r(CV)$	$r(\rho)$
<i>bcd</i>	2	2	2
<i>cad</i>	2	2	2
<i>eve</i>	3	3	3
<i>gt</i>	3	3	3

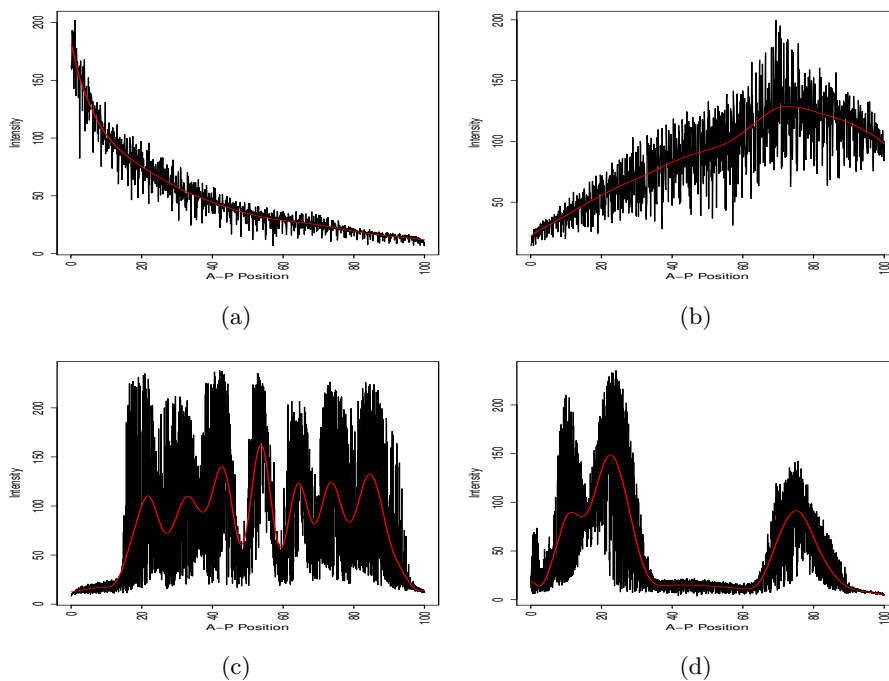


Figure 4: Original (black) and extracted signal (red); (a): *bcd*, (b): *cad*, (c): *gt*, (d): *eve*.

210 Taking a closer look at Fig 4, it is imperative to note that the extracted
 211 signal profiles of *eve* and *gt* do not follow the expression data satisfactorily
 212 when the data series changes sharply. Therefore, in order to solve this issue
 213 and capture the peaks of the profiles, we used sequential SSA. The main idea
 214 underlying this approach is to apply SSA recursively on the residuals with
 215 different window length L [23]. By doing so we extract some components of
 216 the initial series using basic SSA and then extract the remaining components
 217 related to the signal by applying SSA on residuals. Such a recursive SSA
 218 application produces a gradual extraction of the signal present in the noise.
 219 Fig 5 shows the result after applying sequential SSA. As can be seen signal
 220 extraction and peak capturing has been improved accordingly.

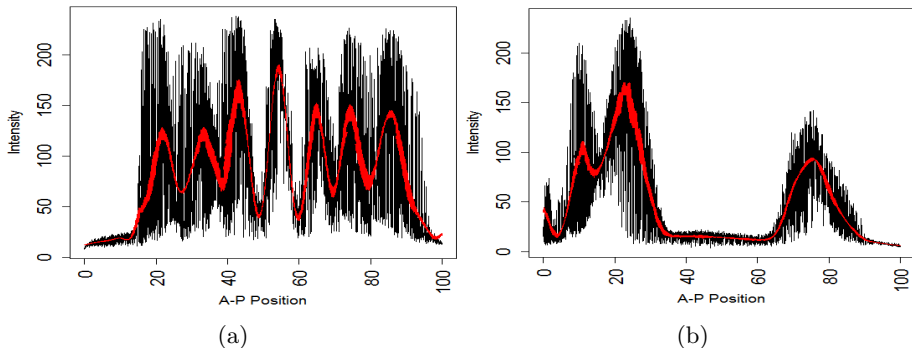


Figure 5: Improving signal extraction using sequential SSA. Original (black) and extracted signal (red);(a): *eve*, (b): *gt* .

221 4 Conclusion

222 In this study, a new approach for removing noise and signal extraction in four
 223 different *Drosophila* segmentation genes was applied. The approach is based
 224 on the distribution of the eigenvalues of a scaled Hankel matrix. The skewness
 225 and variation coefficients of the eigenvalue distribution was used as a new criteria
 226 and indicator for the cut-off point in the eigenvalue spectra between signal
 227 and noise components. The results confirm that the proposed approach gives
 228 a promising output for the gene expression signal extraction and also indicates
 229 that the method used for removing noise from the protein profile of gene ex-
 230 pression should be flexible enough for different type of genes, as in this study
 231 we have obtained different number of eigenvalues needed for signal extraction
 232 in each gene.

233 References

- 234 [1] Porcher A, Dostatni N. The bicoid morphogen system. *Current Biol-*
 235 *ogy*.2010; **20**(5): 249-254.

- 236 [2] Houchmandzadeh B, Wieschaus E, Leibler S. Establishment of developmen-
237 tal precision and proportions in the early *Drosophila* embryo. *Nature*. 2002;
238 **415**: 798-802.
- 239 [3] Alexandrov T, Golyandina N, and Spirov A. Singular Spectrum Analysis of
240 gene expression profiles of early *Drosophila* embryo: exponential-in-distance
241 patterns. *Research Letters in Signal Processing*. 2008; **2008**(12): 1-5.
- 242 [4] Myasnikova E, Samsonova M, Kosman D, & Reinitz J. Removal of back-
243 ground signal from in situ data on the expression of segmentation genes in
244 *Drosophila*. *Development genes and evolution*, 2005; **215**(6): 320-326.
- 245 [5] Surkova S, Kosman D. et al. Characterization of the *Drosophila* segment
246 determination morphome. *Developmental Biology*. 2007; **313**: 844-862.
- 247 [6] Holloway DM, Harrison LG, Kosman D, Vanario Alonso CE, Spirov AV.
248 Analysis of pattern precision shows that *Drosophila* segmentation develops
249 substantial independence from gradients of maternal gene products. *Devel-*
250 *opmental Dynamics*. 2006; **235**(11): 2949-2960.
- 251 [7] Hassani H. Singular Spectrum Analysis: Methodology and Comparison
252 .*Journal of Data Science*. 2007; **5**:239-257.
- 253 [8] Holloway DM, Harrison LG. et al. Analysis of Pattern Precision Shows That
254 *Drosophila* Segmentation Develops Substantial Independence From Gradi-
255 ents of Maternal Gene Products. *Developmental Dynamics*. 2006; **235**: 2949-
256 2960.
- 257 [9] Alexandrov T. A method for trend extraction using Singular Spectrum
258 Analysis. *Revstat*. 2009; **7**(1): 1-22.
- 259 [10] Golyandina NE, Holloway DM, Lopesc, FJP et al. Measuring gene ex-
260 pression noise in early *Drosophila* embryos: nucleus-to-nucleus variability.
261 *International Conference on Computational Science*. 2012; **9**: 373-382.
- 262 [11] Spirov AV, Golyandina NE, Holloway, DM et al. Measuring Gene Expres-
263 sion Noise in Early *Drosophila* Embryos: The Highly Dynamic Compartmen-
264 talized Micro-environment of the Blastoderm Is One of the Main Sources of
265 Noise. *Evolutionary Computation, Machine Learning and Data Mining in*
266 *Bioinformatics*. 2012; **7246**:177-188
- 267 [12] Holloway DM, Lopes FJP, da Fontoura Costa L et al. Gene Expression
268 Noise in Spatial Patterning: hunchback Promoter Structure Affects Noise
269 Amplitude and Distribution in *Drosophila* Segmentation. *PLoS Computa-*
270 *tional Biology*. 2011; **7**(2): e1001069. doi:10.1371/journal.pcbi.1001069
- 271 [13] Hassani H, Ghodsi Z. Pattern Recognition of Gene Expression with Sin-
272 gular Spectrum Analysis. *Medical Sciences*.2014; **2**(3): 127-139.
- 273 [14] Hassani H, Alharbi N, and Ghodsi M. A short Note on the Pattern of
274 Singular Values of a Scaled Random Hankel Matrix. *International Journal*
275 *of Applied Mathematics*. 2014; **27**(3): 237-243.

- 276 [15] Hassani H, Alharbi N, and Ghodsi M. A Study on the Empirical Distribu-
277 tion of the Scaled Hankel Matrix Eigenvalues. *Journal of Advanced Research*.
278 2014; doi:10.1016/j.jare.2014.08.008
- 279 [16] Ghodsi M, Alharbi N, and Hassani H. The Emperical Distribution of the
280 Singular Values of a Random Hankel Matrix. *Fluctuation and Noise Letters*.
281 2015; **14**(3).
- 282 [17] Hassani H, Alharbi N, and Ghodsi M. Distinguishing Chaos from Noise: A
283 New Approach. *International Journal of Energy and Statistics*. 2014; **2**(2):
284 137-150.
- 285 [18] Ghodsi Z, Silva E S, and Hassani, H. Bicoid Signal Extraction with a Se-
286 lection of Parametric and Nonparametric Signal Processing Techniques. *Ge-*
287 *nomics, proteomics & bioinformatics*. 2015; doi:10.1016/j.gpb.2015.02.006.
- 288 [19] Golyandina N, Nekrutkin V, and Zhigljavsky A. *Analysis of Time Series*
289 *Structure: SSA and Related Techniques*. Chapman and Hall/CRC. 2001.
- 290 [20] Available online: <http://urchin.spbcas.ru/flyex/> (accessed on Feburary
291 2014).
- 292 [21] Grimm O, Coppey M, Wieschaus E. Modelling the Bicoid gradient. *De-*
293 *velopment*. 2010; **137**(14): 2253-2264.
- 294 [22] Golyandina N, and Zhigljavsky A. *Singular Spectrum Analysis for Time*
295 *Series*. Springer Briefs in Statistics. Springer. 2013.
- 296 [23] Lahiri K, Vaughan D R, and Wixon B. Modeling SSA's sequential dis-
297 ability determination process using matched SIPP data. *Social Security Bul-*
298 *letin*.1995; **58**: 3.